Int. J. Electrochem. Sci., 7 **(2012)** 6771 - 6786

International Journal of
ELECTROCHEMICAL
SCIENCE
www.electrochemsci.org

Rigorous Characterization of the Facilitated Ion Transfer at Ities in Normal Pulse Voltammetry. Comparison with the Approximated Treatments

E. Torralba[1], *A. Molina*[1,*], *C. Serna*[1], *J. A. Ortuño*[2]

[1] Departamento de Química Física
[2] Departamento de Química Analítica
Facultad de Química, Universidad de Murcia, 30100 Murcia, Spain. Regional Campus of Excellence, Campus Mare Nostrum
[*]E-mail: amolina@um.es

Received: 11 May 2012 / *Accepted:* 28 June 2012 / *Published:* 1 August 2012

Facilitated Ion Transfer (FIT) processes taking place through a complexation reaction in the organic phase have been studied from a rigorous analytical solution valid for any value of the forward and backward kinetic constants of the complexation reaction. The influence of the different parameters on the normal pulse voltammetric (NPV) response and on the half-wave potential of the FIT is discussed. The validity of three interesting approximated solutions is checked by comparison with the rigourous results. Finally, the difference between the NPV voltammograms in presence and absence of ligand is presented as a suitable criterion to characterize the FIT process.

Keywords: Facilitated Ion Transfer, liquid/liquid interfaces, EC mechanism

1. INTRODUCTION

Ion transfer (IT) at liquid-liquid interfaces is a heterogeneous physicochemical process with important implications in electrochemistry, analytical chemistry and membrane sciences, among other areas [1, 2]. Most liquid-liquid systems in which ion transfer takes place consist of an aqueous phase and an organic phase. Ion transfer from the aqueous to the organic phase can be promoted by a ligand initially present in the organic phase which forms a complex with the ion in this phase [3-6]. The Gibbs energy value corresponding to this facilitated ion transfer (FIT) can be much lower than that corresponding to the simple ion transfer (without ligand). Ligands can act as mobile ion carriers in biological or artificial membranes. Since they facilitate the transport of ion across membranes they act as type of ionophores. A condition for this is that the ion binding is reversible. Ionophores can disrupt

membrane ion concentration gradients required for the proper functioning of microorganisms, which convert them into antibiotic agents [7].

Based on this principle and on a proper selection of selective ionophores, many potentiometric [8] and some amperometric ion-selective electrodes [9, 10] for different target ions have been reported. The analytical performance of these sensors is influenced by the complexation constant between the ion and the ionophore and by the selectivity of the complexation reaction. Natural ionophores used in the transport of ions through cell membranes were used first [11]. One group of these are polyethers, which have the ability to transport cations across plasma membranes, which leads to depolarization and cell death [12]. Nowadays, many synthetic ionophores are available for the development of ions sensors and as antimicrobial agents.

The mechanisms proposed for the facilitated ion transfer are analogous to those known for electron transfer at metal electrodes. The ion transfer followed by complexation in the organic phase (TOC) corresponds to the EC mechanism with the ion transfer as the electrochemical step. The aqueous complexation followed by the transfer of the complex ion (ACT) is analogous to the CE mechanism. Finally, the ion transfer with interfacial complexation (TIC) is often considered analogous to the E mechanism [13].

A study of the ion transfer facilitated by complexation in the organic phase (TOC) was carried out in a previous paper [14]. It was found that under certain conditions the TIC mechanism can be obtained as a limiting case of the TOC. In this paper, the influence of the thermodynamic and kinetic parameters of the complexation reaction on the facilitated ion transfer response corresponding to the TOC mechanism has been studied from a rigourous solution valid for any value of the kinetic constants of the complexation reaction (k_1 and k_2). Normal pulse voltammograms at different conditions are presented to illustrate the influence of the different parameters in the electrochemical response and in the half-wave potential. Moreover, the difference between the NPV voltammograms for the facilitated ion transfer and for the single ion transfer is introduced. Interestingly, this displays a peak shape under some conditions, which makes the interpretation of the results clearer.

2. THEORY

Let us consider the reversible transfer of an ion X^+ from an aqueous solution (*W*) to an organic one (*M*), which is facilitated by a highly lipophilic neutral ligand, *L*, present only in the organic phase, according to the following Scheme

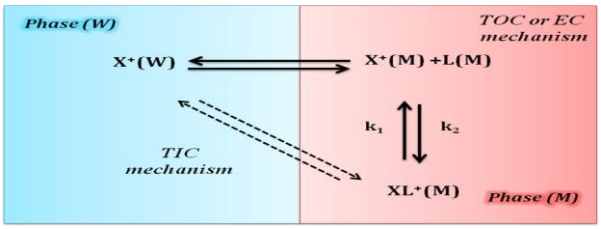

Scheme 1. Schematic view of the facilitated ion transfer processes taking place through a complexation reaction in the organic phase.

where k_1 and k_2 are the forward and backward rate constants of the organic complexation reaction, which is supposed as pseudo-first order with respect to the metal X^+ in the organic phase.

When a constant potential, *E*, is applied to this system and the uptake process establishes a fixed ratio of concentrations of the species involved on both sides of the interfacial region, mass transport can be described by the following diffusive-kinetic equation system and boundary value problem:

$$\left.\begin{aligned}
&\frac{\partial c^W_{X^+}(x,t)}{\partial t} = D^{W_1}_{X^+}\frac{\partial^2 c^W_{X^+}(x,t)}{\partial x^2}\\
&\frac{\partial c^M_{X^+}(x,t)}{\partial t} = D^M_{X^+}\frac{\partial^2 c^M_{X^+}(x,t)}{\partial x^2} - k_1 c^M_{X^+}(x,t) + k_2 c^M_{XL^+}(x,t)\\
&\frac{\partial c^M_{XL^+}(x,t)}{\partial t} = D^M_{XL^+}\frac{\partial^2 c^M_{XL^+}(x,t)}{\partial x^2} + k_1 c^M_{X^+}(x,t) - k_2 c^M_{XL^+}(x,t)
\end{aligned}\right\} \quad (1)$$

$$\left.\begin{aligned}
&t=0, \quad x\le 0\\
&t\ge 0, \quad x\to -\infty
\end{aligned}\right\} \quad c^W_{X^+}(x,0) = c^W_{X^+}(-\infty,t) = c^*_{X^+} \quad (2)$$

$$\left.\begin{aligned}
&t=0, \quad x\ge 0\\
&t\ge 0, \quad x\to \infty
\end{aligned}\right\} \quad \begin{aligned}
&c^M_{X^+}(x,0) = c^M_{X^+}(\infty,t) = 0\\
&c^M_{XL^+}(x,0) = c^M_{XL^+}(\infty,t) = 0
\end{aligned} \quad (3)$$

$x=0,\ t>0$

$$D^W_{X^+}\left(\frac{\partial c^W_{X^+}(x,t)}{\partial x}\right)_{x=0} = D^M_{X^+}\left(\frac{\partial c^M_{X^+}(x,t)}{\partial x}\right)_{x=0} \quad (4)$$

$$D^M_{XL^+}\left(\frac{\partial c^M_{XL^+}(x,t)}{\partial x}\right)_{x=0} = 0 \quad (5)$$

$$c^M_{X^+}(0,t) = c^W_{X^+}(0,t)e^{\eta} \quad (6)$$

with

$$\eta = \frac{F}{RT}\left(E - \Delta^W_M \phi^{0'}_{X^+}\right) \quad (7)$$

where $c^p_i(x,t)$ and D^p_i are, respectively, the concentration of the species *i* in phase *p* (*i* = X^+, XL^+; *p* = *W*, *M*) and its diffusion coefficient, and $c^*_{X^+}$ and $\Delta^W_M \phi^{0'}_{X^+}$ are the initial concentration of the ion X^+ and its formal ion transfer potential. Other symbols have their usual meaning.

By following a mathematical procedure similar to that described in reference [15] and assuming $D^M_{X^+} = D^M_{XL^+} = D^M$ we can solve the above problem, obtaining the following rigorous solution for the current corresponding to the FIT process

$$\frac{I}{I_d} = \frac{\gamma e^{\eta}}{1+\gamma e^{\eta}} - \frac{\sqrt{\pi}}{2} S^{FIT} \tag{8}$$

where

$$\gamma = \sqrt{\frac{D^M}{D^W_{X^+}}} \tag{9}$$

$$S^{FIT} = \sum_{j=1}^{\infty} a_j \chi^j \tag{10}$$

$$I_d = zFA\sqrt{\frac{D^W_{X^+}}{\pi t}}\, c^*_{X^+} \tag{11}$$

and the coefficients a_j in Eq. (10) are given by

$$a_0 = \frac{p_0}{1+\gamma e^{\eta}} \tag{12}$$

$$a_j = \frac{1}{(1+K)(1+\gamma e^{\eta})}\left[\frac{\gamma K e^{\eta} a_0}{j!}\left(p_0 - p_{2j}\right) - \sum_{n=1}^{j-1}\frac{a_n}{(j-n)!}\left(p_{2j}\left[1+\gamma e^{\eta}(1+K)\right] + p_{2n}K\right)\right] \;;\; j \geq 1 \tag{13}$$

with

$$\left.\begin{aligned} p_j &= \frac{2\Gamma\left(1+\frac{j}{2}\right)}{\Gamma\left(\frac{1+j}{2}\right)} \quad ; \quad j \geq 0 \\ \Gamma &\equiv \text{ Euler Gamma function} \end{aligned}\right\} \tag{14}$$

In the above expressions, K is the stability constant of the complex under the pseudo-first-order assumption

$$K = K' c^*_L(M) = \frac{k'_1 c^*_L(M)}{k_2} = \frac{k_1}{k_2} = \frac{c^*_{XL^+}(M)}{c^*_{X^+}(M)} \tag{15}$$

with $c_i^*(M)$ being the equilibrium concentrations at phase M ($i = X^+, XL^+, L$), and χ is the dimensionless rate constant of the organic complexation reaction

$$\chi = \kappa t \tag{16}$$

with

$$\kappa = k_1 + k_2 \tag{17}$$

Equation (8) holds for any χ value. However, for $\chi \geq 15$, the convergence of S^{FIT} series (Eq. (10)) is too slow and it is convenient to use the kinetic steady state approximation, which behaves exactly as the rigourous solution for these χ values.

2.1. Kinetic steady state approximation (kss)

Considering that the kinetics of the homogeneous chemical reaction are fast enough ($(k_1 + k_2)t \geq 5$) the *kss* approximation applies with an error of less than 1.5 mV (see results and discussion). This approximation relies on the perturbation of the chemical equilibrium being independent of time $\left(\partial\phi(x,t)/\partial t = 0\right.$; with $\left.\phi(x,t) = \left[Kc_{X^+}^M(x,t) - c_{XL^+}^M(x,t)\right]e^{\chi}\right)$ [16, 17]. Under *kss* conditions the following expression for the current corresponding to the FIT can be derived [14]

$$\frac{I_{kss}}{I_d} = \frac{\gamma e^{\eta}(1+K)}{1+\gamma e^{\eta}(1+K)} F\left(\chi^{kss}\right) \tag{18}$$

with

$$\chi^{kss} = \frac{2\sqrt{\chi}}{K}\left(1+\gamma e^{\eta}(1+K)\right) \tag{19}$$

$$F(x) = \sqrt{\pi}\frac{x}{2}e^{(x/2)^2} erfc\left(\frac{x}{2}\right) \tag{20}$$

and η, K and χ being given by Eqs. (7), (15) and (16), respectively.

2.2. Diffusive-kinetic steady state approximation (dkss).

When $\chi^{kss} \geq 21.5$, the diffusive-kinetic steady state (*dkss*) approximation applies [16, 17]. Under these conditions, $F\left(\chi^{kss}\right) = \sqrt{\pi}\chi^{kss} / \left(2 + \sqrt{\pi}\chi^{kss}\right)$ and Eq. (18) for the I/E response simplifies to

$$\frac{I_{dkss}}{I_d} = \frac{\gamma e^{\eta}(1+K)}{1+K/\sqrt{\pi\chi}+\gamma e^{\eta}(1+K)} \qquad (21)$$

This response is easier to handle than the previous ones, and can be linearized in an identical way to that corresponding to a simple ion transfer process, so we have

$$E = E^{1/2} + \frac{RT}{F}\ln\left(\frac{I_{dkss}}{I_d - I_{dkss}}\right) \qquad (22)$$

with $E^{1/2}$ being the half-wave potential for the facilitated ion transfer, given by [14]

$$E^{1/2} = \Delta_M^W \phi_{X^+}^{0'} + \frac{RT}{F}\ln\left(\frac{1}{\gamma}\right) + \frac{RT}{F}\ln\left(\frac{1+K/\sqrt{\pi\chi}}{1+K}\right) \qquad (23)$$

As we showed in a previous paper [14], this expression can be very useful for obtaining K and χ for the chemical complexation avoiding numerical fitting.

2.3. Total equilibrium conditions (te).

If the rates of the complex formation and dissociation processes are sufficiently large in comparison to the diffusion rate so as to consider that the complex formation and dissociation are at equilibrium even when current is flowing, the total equilibrium approximation (*te*) applies [14]. The expression for the *I/E* curve under *te* conditions can be obtained by making ($\chi\left(=\left(k_1+k_2\right)t\right)\to\infty$) in Eqs. (18) or (21)

$$\frac{I_{te}}{I_d} = \frac{\gamma e^{\eta}(1+K)}{1+\gamma e^{\eta}(1+K)} \qquad (24)$$

The minimum χ value necessary to satisfy this simple equation depends on the value of the equilibrium constant of the complexation reaction (see Table 1 in results and discussion).

The half-wave potential in this limiting case is given by [14]

$$E^{1/2} = \Delta_M^W \phi_{X^+}^{0'} + \frac{RT}{F}\ln\left(\frac{1}{\gamma}\right) + \frac{RT}{F}\ln\left(\frac{1}{1+K}\right) \qquad (25)$$

The *te* approximation leads to the FIT processes commonly known as TIC reactions (Transfer by Interfacial Complexation), which are the most widely studied FIT mechanisms. The complexation-descomplexation in this kind of FIT processes occurs so fast that they are often regarded as an E

mechanism which exhibits dependence on the equilibrium constant of the organic complexation K [18].

3. RESULTS AND DISCUSSION

The effects of the kinetics and of the equilibrium constant of the complexation reaction in the rigorous NPV response of the FIT are studied in Figure 1. We plot the normalized *I/E* curves obtained from the rigorous solution (Eq. (8) for $\chi \leq 15$ and Eq. (18) otherwise) for a fixed value of the equilibrium constant K and different values of the dimensionless kinetic parameter $\chi\left(=\left(k_1+k_2\right)t\right)$ (Figure 1a) and vice versa (Figure 1b).

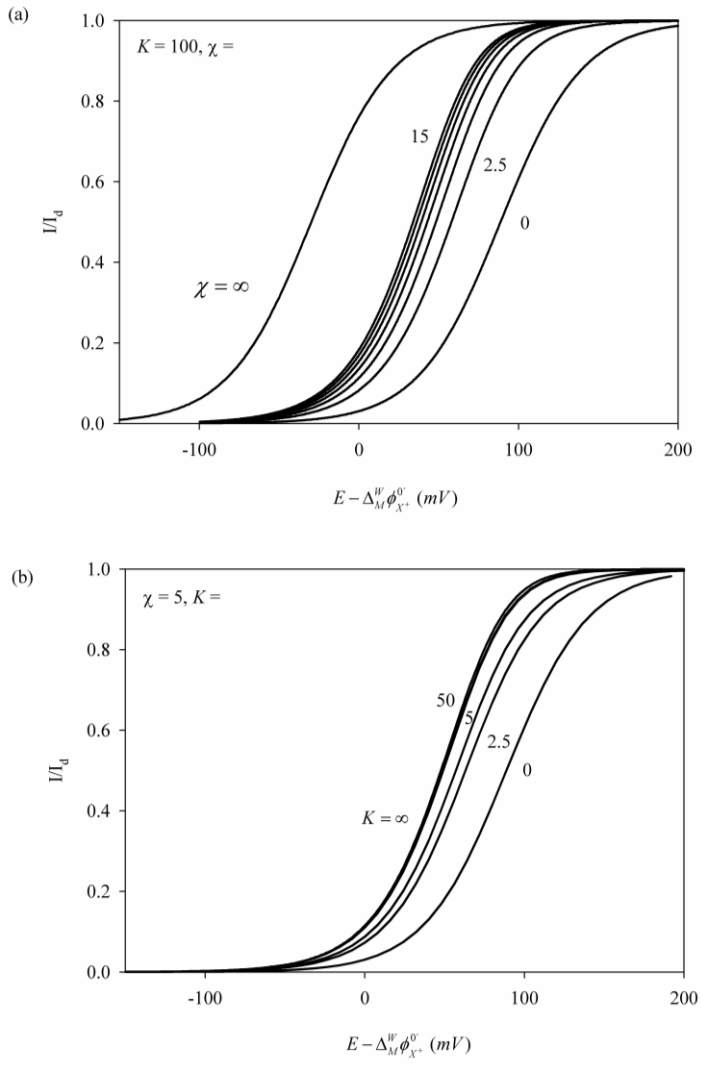

Figure 1. Normalized rigorous *I/E* curves, obtained from Eq. (8) for $\chi \leq 15$ and Eq. (18) for $\chi > 15$, for a fixed value of the equilibrium constant K and different values of the dimensionless kinetic parameter χ (Figure 1a) and vice versa (Figure 1b). χ and K values are given on the curves. $D_{X^+}^{W} = 10^{-5}$ cm^2 s^{-1}, $D_{X^+}^{M} = 10^{-8}$ cm^{2}s^{-1}.

As can be seen, an increase of χ or K leads to a shift of the rigourous I/E curves to lower potentials, since the ion transfer become easier on account of an enhancement of the ion demand at the organic interface surroundings.

The current varies between two extreme situations with χ and K:

- Regarding the influence of χ (Figure 1a), these situations correspond to the case of inert equilibrium ($\chi \to 0$) given by

$$\frac{I}{I_d} = \frac{\gamma e^{\eta}}{1+\gamma e^{\eta}} \tag{26}$$

which can be obtained directly from Eq. (8) and is identical to that corresponding to a simple IT [19], and the situation corresponding to total equilibrium conditions ($\chi \to \infty$) given by Eq. (24). Note that small χ values are the result of organic complexation reactions with slow kinetics, short experiment time, or very low ligand concentration (see Eqs. (15)-(17)), and in constrast, high χ values can be attributed to fast organic complexation reactions, long experiment durations or very high ligand concentration in the organic phase.

- With respect to the influence of K (Figure 1b), the I/E curve shift with this parameter from an equilibrium totally displaced toward the ion ($K \to 0$), which also correspond to a simple IT (Eq. (26)) to a totally displaced toward the complex equilibrium or irreversible organic complexation ($K \to \infty$). The *I/E* expression in this last limiting situation can be obtained easily by making $K \to \infty$ in Eq. (8) and in Eq. (18) for $\chi \geq 15$,

$$\left.\begin{array}{ll} \dfrac{I_{K\to\infty}}{I_d} = \dfrac{\gamma e^{\eta}}{1+\gamma e^{\eta}} - \dfrac{\sqrt{\pi}}{2} S_{K\to\infty}^{FIT} & for \quad \chi \leq 15 \\ \dfrac{I_{K\to\infty}}{I_d} = F\left(\chi_{K\to\infty}^{kss}\right) & otherwise \end{array}\right\} \tag{27}$$

$$S_{K\to\infty}^{FIT} = \sum_{j=1}^{\infty} a_{j,(K\to\infty)} \chi^{j} \tag{28}$$

$$a_{j,(K\to\infty)} = \frac{1}{1+\gamma e^{\eta}} \left[\frac{\gamma e^{\eta} a_0}{j!} \left(p_0 - p_{2j} \right) - \sum_{n=1}^{j-1} \frac{a_n}{(j-n)!} \left(p_{2j} \gamma e^{\eta} + p_{2n} \right) \right] \quad ; \quad j \geq 1 \tag{29}$$

$$\chi_{K\to\infty}^{kss} = 2\sqrt{\chi} \gamma e^{\eta} \tag{30}$$

and a_0, p_j, χ and $F\left(x\right)$ given by Eqs.(12), (14), (16) and (20), respectively.

In Figure 2 we compare the rigurous solution (Eq.(8)) with the different approximations. Thus, we have plotted the *I/E* curves obtained from the rigorous treatment (solid black line) and those of the *kss* (dash line), *dkss* (dotted lines) and total equilibrium (dash-dotted lines) approximations for two fixed values of K (K=1 for Figures a-d and K=10^3 for Figures e-h) and different values of χ (given on the curves).

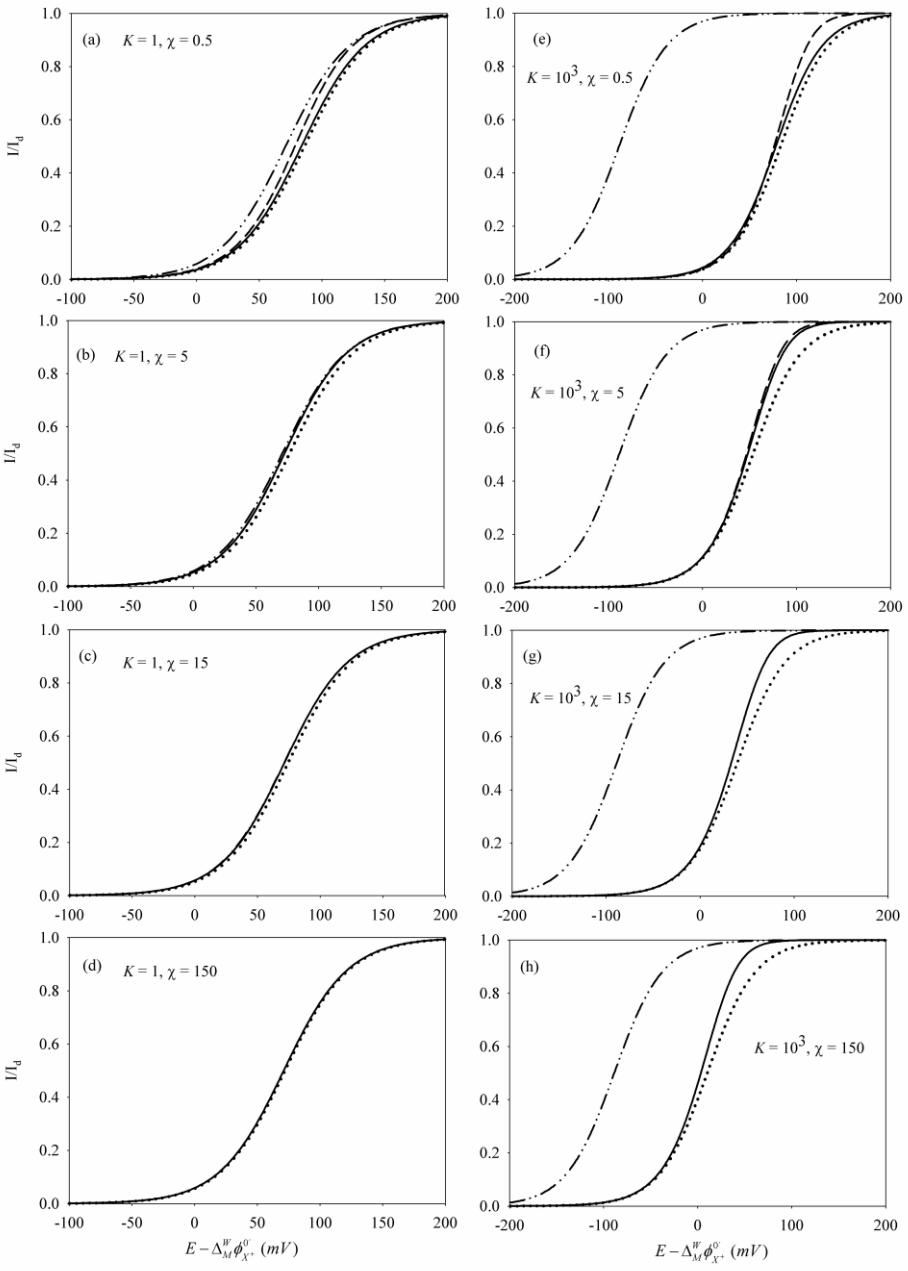

Figure 2. Normalized *I/E* curves corresponding to the rigorous solution (solid lines, obtained from Eq. (8) for $\chi \leq 15$ and Eq. (18) otherwise), and the *kss* (dashed lines, Eq. (18)), the *dkss* (dotted lines, Eq. (21)) and *te* (dash-dotted lines, Eq. (24)) approximations, for different values of χ and K (given on the curves). $D^W_{X^+} = 10^{-5}$ cm^2 s^{-1}, $D^M_{X^+} = 10^{-8}$ cm^{2}s^{-1}.

From any of the Figures presented it can be seen immediately that except for very small values of χ (χ = 0.5 in Figures a and e) the *kss* curves (Eq. (18)) and the rigorous curves (Eq. (8)) practically overlap whatever the *K* value. Therefore, the *kss* approximation will be used instead of the rigorous expression for $\chi \geq 5$.

Regarding the goodness of the *dkss* and *te* approximations, it is clear from Figure 2 that their reliability depends on the K and χ values. In the case of the *dkss* approximation, we can see that the *I/E* curves adjusts properly to the rigorous curves for any χ value when small K values are considered (K = 1 in Figures a-d); for high K values (K = 10^3 in Figures e-h) the error in the measurement of the half-wave potentials is as maximum up to of 7 mV (see also Figure 3).

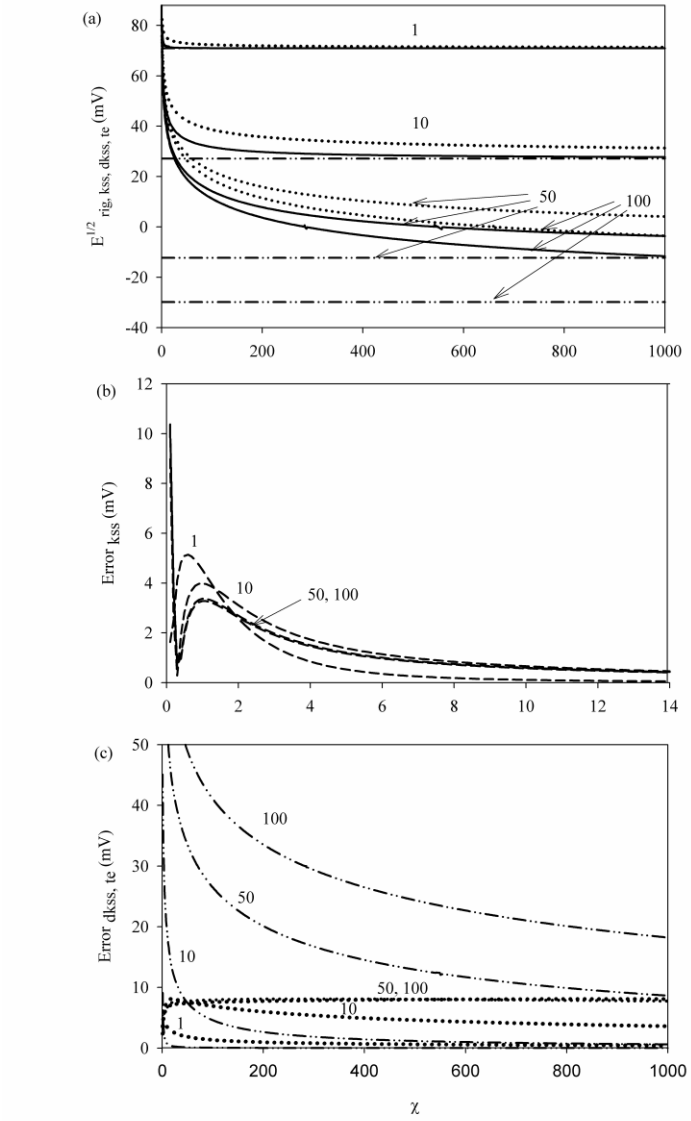

Figure 3. **3a:** $E^{1/2}$ *vs* χ curves obtained from the rigorous solution (solid lines, obtained numerically from Eq. (8) for $\chi \leq 15$ and Eq. (18) otherwise), and from the *kss* (dashed lines, obtained numerically from Eq. (18)), the *dkss* (dotted lines, obtained from Eq.(23)) and *te* (dash-dotted lines, Eq.(25)) approximations, for different values of K (given on the curves). 3b and 3c: Absolute error curves corresponding to the *kss* (dashed lines), *dkss* (dotted lines) and *te* (dash-dotted lines) approximations. $\Delta_M^w \phi_{X^+}^{0'}$ = 0 mV, $D_{X^+}^W = 10^{-5}$ cm^2 s^{-1}, $D_{X^+}^M = 10^{-8}$ cm^{2}s^{-1}.

On the other hand, the position of the total equilibrium curves shows a large shift with K with respect to the rigourous curve in the conditions selected (compare the rigourous and *te* curves with K =1 and K =10^3), in such a way that for the range of χ values selected ($0.5 \le \chi \le 150$) the *te* approximation quickly losses reliability as K increases (see also Figure 3). The error in the measurement of the half-wave potentials for K =10^3 is around 100 mV when using this aproximation, so in these conditions the *te* approximation should not be used.

From these Figures it can be concluded that for relatively small χ values ($0.5 \le \chi \le 150$) the *dkss* approximation could be used instead of the *kss* or rigorous one for a general good description of the system, avoiding numerical fitting whatever the K value, whereas the *te* approximation is only applicable for weak complexes (specifically, for complexes with $K \le 15$). To obtain more accurate results the *kss* or rigorous solutions are required.

Figure 3a depicts the evolution of the half-wave potential obtained from the rigorous solution (black solid lines), and from the *kss* (dashed lines), *dkss* (dotted lines) and *te* (dash-dotted lines) approximations with the dimensionless rate constant χ for a range of χ values located between 0 and 1000 for different values of the equilibrium constant K (shown on the curves). In order to check the validity of the different approximate solutions in these conditions by comparison with the rigorous results, in Figures 3b and 3c the absolute error of the *kss*, *dkss* and *te* approximations are shown for the different K values selected.

From the rigorous curves depicted in Figure 3a (solid black lines) we can see that $E^{1/2}$ shifts toward lesser values with χ and with K, that is, as the metal complex interconversion become faster and as the chemical complexation becomes more irreversible, respectively. With respect to the limiting values taken by $E^{1/2}$, we can distinguish those corresponding to very slow kinetics or inert equilibrium ($\chi \to 0$ and/or $K \to 0$), both of which correspond to the simple ion transfer [19]

$$E^{1/2} = \Delta_M^W \phi_{X^+}^{0'} + \frac{RT}{F} \ln\left(\frac{1}{\gamma}\right) \qquad (31)$$

and also those corresponding to the case of very fast kinetics ($\chi \to \infty$) and irreversible complexation reactions ($K \to \infty$), which depend on K and χ, respectively. Indeed, as can be seen from the Figure, for a given K value $E^{1/2}$ decreases as χ increases until it reaches the limiting value given by Eq. (25) which depends on K. In the same way, for a given value of χ $E^{1/2}$ decreases as K increases until reach its limiting value when the complexation reaction becomes irreversible.

Note that the *kss* curves in Figure 3a overlap with the rigorous ones except for very small χ values, and so their differences are not noticeable in the χ scale selected.

From the error curves presented in Figure 3b we can see that the *kss* approximation (dashed lines) can be used reliably for $\chi \ge 5$, since it leads to errors lesser that 1.5 mV (see also the *I/E* curves presented in Figure 2). Notwithstanding, some precautions must be taken in order to apply *dkss* and *te* approximations. From the curves depicted in Figure 3a we can see that, in general, for the different K values presented, the $E^{1/2}$ given by the *dkss* approximation (Eq. (23)) follows the same trend with χ as the rigorous one, with the fit being better for the curves corresponding to weaker organic complexes

(K =1 and 10 in the Figure). Nevertheless, the error in the quantification of $E^{1/2}$ does not exceed 8 mV for any of the K values presented. With respect to the *te* approximation, it is totally inadequate to quantify $E^{1/2}$ within the range of χ values presented as can be seen for the dash-dotted curves presented in Figure 3a. The error committed with this approximation is much higher than that corresponding to the *dkss* one, and it increases very quickly with the strength of the complex formed in the organic phase (see the curves in Figure 3c).

The error curve corresponding to the *te* approximation decays quickly with χ (see Figure 3c). Table 1 gathers the $\chi(te)_{\lim}$ values above which the *te* approximation can be used besides the *dkss* one for a qualitative good description of the system under study, and which correspond to the χ value above which the difference between $E^{1/2}$ rigorous and $E^{1/2}$ approximated is less than 8 mV.

Table 1. χ values above which the *te* approximation is applicable.

K	$\chi_{\lim}(te)$
0.5	--
1	1.26
5	12.6
10	50
50	1259
100	5012
200	$2.0\cdot10^{4}$
500	$1.3\cdot10^{5}$
1000	$5.1\cdot10^{5}$
2000	$2.0\cdot10^{6}$
5000	$1.2\cdot10^{7}$
10^{4}	$5.0\cdot10^{7}$
$5.0\cdot10^{4}$	$2.0\cdot10^{8}$

For a given equilibrium constant K, for χ values lesser than $\chi_{\lim}(te)$ the *dkss* approximation will be always preferable, but for χ values greater than $\chi_{\lim}(te)$ the *te* expressions (Eqs. (24) and (25)) can be also used. Bear in mind that for quantitative purposes the rigorous or *kss* solutions are needed.

A good criterion to characterize the existence of complexation in the membrane consists in study the behavior of the difference between the *I/E* curves obtained in presence and in absence of ligand, so that they present a peak whose height is sensitive to the kinetic and thermodynamic effects of the complexation reaction. Thus, in Figure 4 we present the normalized $(I_{FIT}-I_{IT})$ *vs* E curves, obtained from Eqs.(8), (18) and (26), for different values of χ and K (shown on the curves).

The peak height of the $(I_{FIT}-I_{IT})$ *vs* E curves is strongly influenced by the equilibrium constant of the complexation reaction, as can be seen from the comparison of the curves presented in Figures 4a-c. Indeed, the K value establishes the range within which the $(I_{FIT}-I_{IT})$ *vs* E curves vary with the dimensionless kinetic constant χ.Thus, the height of the curves increases with χ up to a limit χ value depending on *K*. For weaker complexes ($K=1$ in Figure 4a), the $(I_{FIT}-I_{IT})$ *vs* E curves

coincide for $\chi \geq 5$, while for moderately strong complexes ($K = 1000$ in Figure 4b) the peak height is sensitive to the χ value up to $\chi \approx 10^6$.

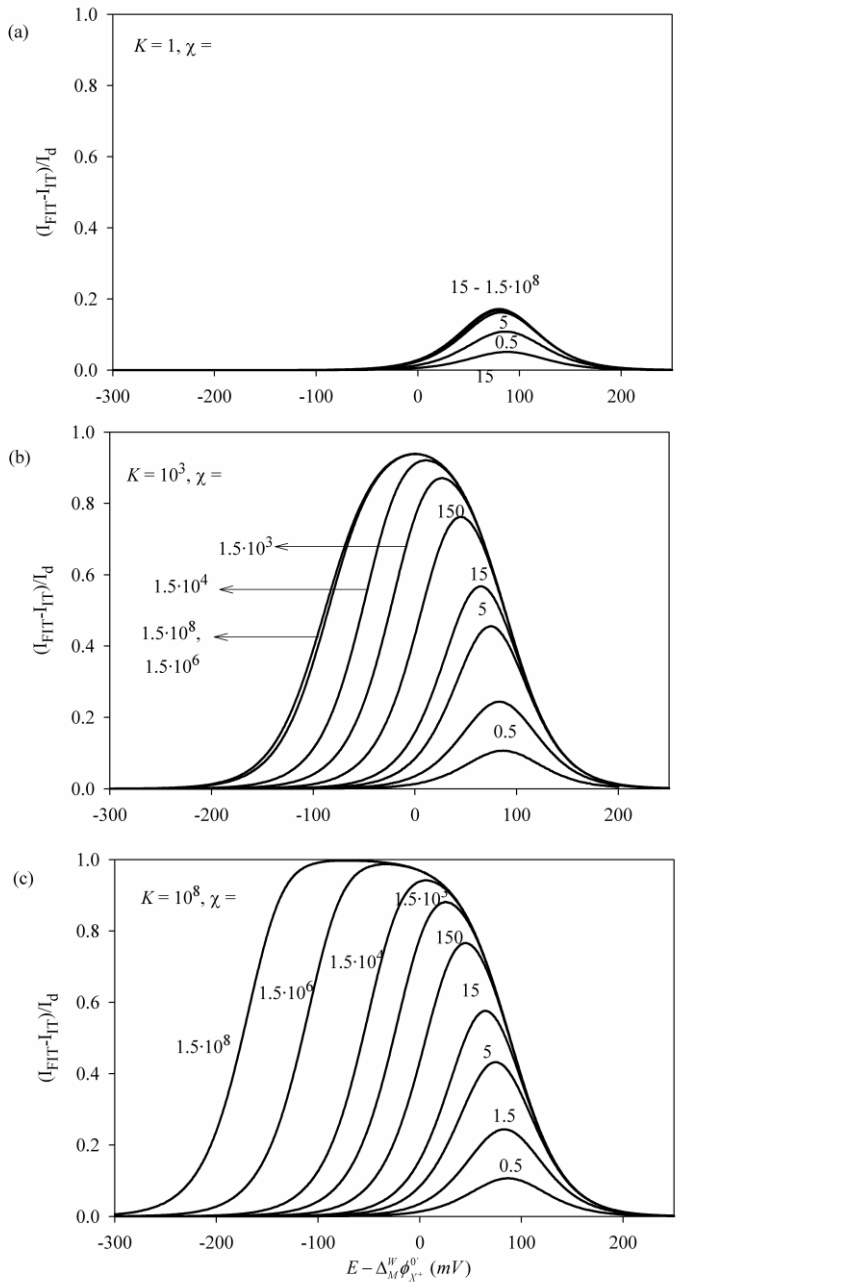

Figure 4. Rigorous normalized $(I_{FIT} - I_{IT})$ *vs* E curves, obtained from Eq. (8) for $\chi \leq 15$, Eq. (18) for $\chi > 15$ and Eq. (26), for different values of χ and K (shown on the curves). $D^W_{X^+} = 10^{-5}$ cm^2 s^{-1}, $D^M_{X^+} = 10^{-8}$ cm^{2}s^{-1}.

For very high complexation constants ($K = 10^8$ in Figure 4c) the $(I_{FIT} - I_{IT})$ vs E curves show a plateau with $(I_{FIT} - I_{IT}) / I_d = 1$ for χ values higher than $1.5 \cdot 10^3$. This is because for very strong

complexes (high K values) and fast complexation reactions (high χ values) the *I/E* wave corresponding to the FIT appears at much lesser potentials than the simple ion transfer wave, and so the difference between the two normalized *I/E* signals is equal to the unity.

The behavior described above suggest the construction of working curves to determinate the kinetic parameters of the system from NPV experiments performed in presence and absence of ionophore in the organic phase, as those presented in Figure 5.

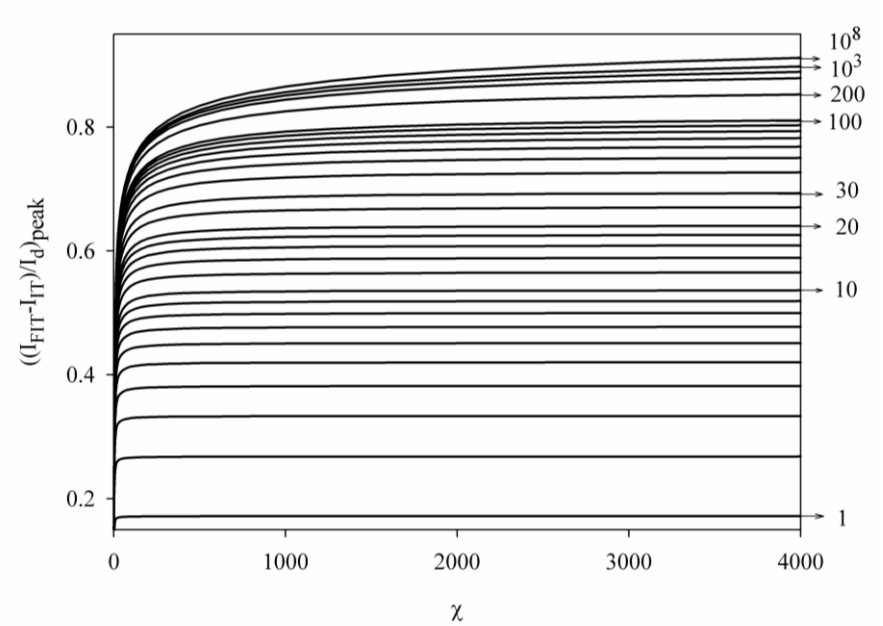

Figure 5. $\left((I_{FIT}-I_{IT})/I_d\right)_{peak}$ *vs* χ curves obtained from the rigorous solution (Eq. (8) for $\chi \leq 15$ and Eq. (18) for $\chi > 15$) and Eq. (26) for different K values (given on the curves). $\Delta_M^w \phi_{X^+}^{0'}$ = 0 mV, $D_{X^+}^W = 10^{-5}$ cm^2 s^{-1}, $D_{X^+}^M = 10^{-8}$ cm^{2}s^{-1}.

From a given K, the value of kinetics of the complexation reaction can be easily obtained from these curves and vice versa. Note that from high χ and small K values the $(I_{FIT}-I_{IT})/I_d$ vs χ curves become insensitive to χ. This is an indication of the attainment of total equilibrium conditions.

4. CONCLUSIONS

- The influence of the thermodynamic and kinetic parameters $\left(K\left(=k_1/k_2\right)\right.$ and $\left.\chi\left(=\left(k_1+k_2\right)t\right)\right)$ of the complexation reaction on the Facilitated Ion Transfer (FIT) responses has been studied from a rigorous solution, valid for any value of the kinetic constants of the complexation reaction (k_1 and k_2). The expressions corresponding to the limiting situations of very weak and very strong complexes, and to very fast or very slow kinetics of the complexation reaction have been deduced.

- The validity of three approximated solutions has been checked by comparison with the rigurous results: the kinetic steady state approximation (*kss*), the diffusive kinetic steady state aproximation (*dkss*), and the total equilibrium aproximation (*te*). From this comparison we have pointed out that the *kss* aproximation can be reliably used instead of the rigorous one for any *K* value when $(k_1 + k_2)t \geq 5$. Moreover, with respect to the more severe *dkss* and *te* approximations, the *dkss* treatment can be used instead of the rigorous solution for a reasonably good qualitative description of the system for any value of χ and *K* values, not involving errors greater than 8 mV. However the *te* treatment is only applicable for fast organic complexation reactions and weak complexes (see Table 1).

- It is shown that the existence of complexation in the membrane can be characterized by studying the behavior of the difference between the *I/E* curves obtained in presence and in absence of ligand on account of the fact that they present a peak of which height is sensitive to the kinetic and thermodynamic effects of the complexation reaction. In this respect, working curves have been proposed to determine the forward and backward kinetic constants of the complexation reaction based on these differences.

ACKNOWLEDGEMENTS

The authors greatly appreciate the financial support provided by the Dirección General de Investigación Científica y Técnica (Project Numbers CTQ2011-27049/BQU and CTQ2009-13023/BQU), and the Fundación SENECA (Project Number 08813/PI/08). Also, E. T. thanks the Ministerio de Ciencia e Innovación for the grant received.

References

1. Z. Samec, *Pure Appl. Chem.*, 76 (2004) 2147.
2. A. Molina, C. Serna, J. A. Ortuño and E. Torralba, *Annu. Rep. Prog. Chem., Sect. C*, 108 (2012) 126.
3. R. Gulaboski, E. S. Ferreira, C. M. Pereira, M. N. D. S. Cordeiro, A Garau, V. Lippolis and A. F. Silva, *J. Phys. Chem. C*, 112 (2008) 153.
4. J. Langmaier and Z. Samec, *Anal. Chem*. 81 (2009) 6382.
5. S. A. Dassie, *J. Electroanal. Chem*, 643 (2010) 20.
6. F. Reymond, P. Carrupt and H. H. Girault, *J. Electroanal. Chem.*, 449 (1998) 49.
7. M. M. Faul and B. E. Huff, Chem. Rev., 100 (2000) 2407.
8. P. Bühlmann, E. Pretsch and E. Bakker, *Chem. Rev.*, 98 (1998) 1593.
9. Z. Samec, E. Samcová and H. H. Girault, *Talanta*, 63 (2004) 21.
10. M. Senda, H. Katano and M. Yamada, *J. Electroanal. Chem*., 468 (1999) 34.
11. J. Koryta, *Electrochim. Acta*, 24 (1978) 293.
12. H. Wang, N. Liu , L. Xi, X. Rong, J. Ruan, and Y. Huang, *Appl. Environ. Microbiol*., doi:10.1128/AEM.02915-10.
13. P. D. Beattie, R. G. Wellington and H. H. Girault, *J. Electroanal. Chem*., 396 (1995) 317.
14. A. Molina, E. Torralba, C. Serna and J. A. Ortuño, *J. Phys. Chem. A*, doi: 10.1021/jp109362.
15. J. Gálvez, A. Serna, A. Molina and D. Marín, *J. Electroanal. Chem*., 102 (1979) 277.

16. A. Molina, I. Morales and M. Lopez-Tenes, *Electrochem. Commun*., 8 (2006) 1062.
17. A. Molina and I. Morales, *Electrochem. Commun*., 8 (2006) 1453.
18. H. Matsuda, Y. Kamada, K. Kanamori, Y. Kudo and Y. Takeda, *Bull. Chem. Soc. Jpn*., 64 (1991) 1497.
19. A. Molina, C. Serna, J. A. Ortuño and E. Torralba, *Int. J. Electrochem. Sci*., 3 (2008) 1081.